Probe-Wavelength Dependence of Picosecond Time-Resolved Anti-Stokes Raman Spectrum of Canthaxanthin: Determination of Energy States of Vibrationally Excited Molecules Generated via Internal Conversion from the Lowest Excited Singlet State

Takakazu Nakabayashi, Hiromi Okamoto, and Mitsuo Tasumi*

Department of Chemistry and Research Centre for Spectrochemistry, School of Science, The University of Tokyo, Bunkyo-ku, Tokyo 113, Japan

Received: October 24, 1996; In Final Form: January 31, 1997[⊗]

The vibrational relaxation process in the ground electronic state (S_0) of canthaxanthin after internal conversion from the lowest excited electronic state (S_1) to the S_0 state is studied by picosecond time-resolved anti-Stokes Raman spectroscopy. The pump-induced intensities of two strong anti-Stokes Raman bands reach their maxima at delay time ∼12 ps from the pump pulse, and decay with a time constant of 15−20 ps. The peak position of the transient "in-phase" C═C stretching anti-Stokes Raman band shows a small shift to a lower frequency from that observed in the stationary (cw) spectrum. In order to determine the energy levels on which the observed vibrationally excited molecules are populated, the probe-wavelength dependence of the pump-induced anti-Stokes Raman intensities are analyzed. Most of the vibrationally excited transients giving rise to the transient 1520 cm^{-1} band at delay time 12 ps are on the first excited vibrational level of the C═C stretching mode in the S_0 state. This result suggests that the intramolecular vibrational redistribution (IVR) process is very fast and contributes only to the rise part of the time dependence of the anti-Stokes Raman intensity. The observed shift of the C═C stretching band is considered to arise from anharmonic coupling with various other vibrational modes which are excited through the IVR process, rather than from contributions of molecules on highly excited levels of the C═C stretching mode generated immediately after the internal conversion from the S_1 state.

Introduction

Knowledge on intramolecular and intermolecular vibrational relaxation processes is of fundamental importance in the study of chemical dynamics. Following photoexcitation and/or nonradiative electronic transition, dissipation of excess vibrational energy proceeds in roughly two steps. Vibrational energy stored on an excited level of a particular mode is first distributed among all intramolecular vibrational modes (intramolecular vibrational redistribution, IVR), and a quasiequilibrium state is created in populations at intramolecular vibrational levels. This randomized vibrational energy then dissipates to the surrounding medium (vibrational cooling, VC).

Kaiser and co-workers have extensively studied vibrational relaxation dynamics by pico- to femtosecond time-resolved pump−probe spectroscopy in the condensed phase.[1] From a number of experimental observations, they have derived a general rule that the typical time scale of IVR is in the subpicosecond range and that of VC in tens of picoseconds for large molecules in solution. However, several recent experiments have suggested that the IVR processes might not be completed within a few picoseconds in some cases.[2−13] For example, time-resolved absorption spectra observed for nascent *trans*-stilbene in the ground electronic state (S_0) formed via photoisomerization of *cis*-stilbene[2,3] have shown that the IVR process is not completed in the time range of the *cis* to *trans* photoisomerization (subpicosecond), and nonequilibrium populations persist for several picoseconds. From the anti-Stokes Raman spectral changes of *trans*-stilbene in the lowest excited singlet state (S_1),[4,5] the time scale of the IVR process in the S_1 state has been estimated to be of the order of picoseconds.[4] Experimental results on other polyatomic molecules, namely, bacteriorhodopsin[6,7] porphyrins,[8,9] and 2-(2′-hydroxy-5′-methylphenyl)benzotriazole[10] have also suggested that the IVR processes occur in the picosecond range.

Time-resolved anti-Stokes Raman spectroscopy is useful for monitoring vibrational relaxation dynamics in solution. It probes only those molecules which are populated in excited vibrational states, providing mode-specific information. Recently, several groups[4−9,12,13] have reported the anti-Stokes Raman spectra of molecules in excited vibrational states generated via photoexcitation. In order to clarify dynamical features of the IVR processes, it is essential to determine the energy levels on which the observed vibrationally excited molecules are populated. However, information on this point is limited.

In this paper, we try to obtain information on the energy levels on which vibrationally excited carotenoid molecules are populated, using picosecond time-resolved anti-Stokes Raman spectroscopy. Carotenoids play an important role in photosynthetic systems.[14−17] They act as light-harvesting pigments which transfer the energy of light to photosynthetic reaction centers. They also work as a quencher of chlorophyll in the excited triplet state and oxygen in the excited singlet state. To understand the biochemical functions of carotenoids, it is required to study in detail their excited states and relaxation processes after photoexcitation. The photophysical scheme of carotenoids is shown in Figure 1a. Under irradiation of visible light, carotenoids are excited to an optically allowed, excited singlet state (S_2), and the excited molecules relax from the S_2 state to the S_1 state by rapid internal conversion on the subpicosecond time scale. Optical transition between the S_0 and S_1 states is forbidden by symmetry. The S_1 state has a lifetime of several picoseconds.[14−17] Vibrationally excited carotenoid molecules in the S_0 state are generated via internal conversion from the

* To whom correspondence should be addressed. E-mail: mtasumi@chem.s.u-tokyo.ac.jp.

[⊗] Abstract published in *Advance ACS Abstracts,* April 1, 1997.

S1089-5639(96)03303-8 CCC: $14.00

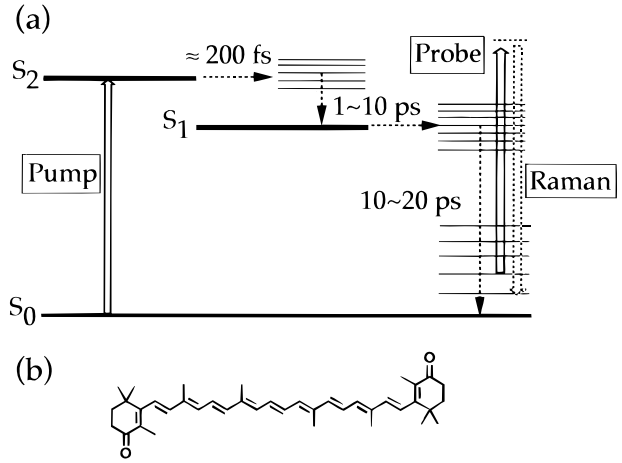

Figure 1. (a) Photophysics of a carotenoid molecule and the experimental scheme of picosecond time-resolved anti-Stokes Raman spectroscopy. A pump pulse excites a carotenoid molecule, and the anti-Stokes Raman spectrum of vibrationally excited S_0 state of the carotenoid is obtained by a probe pulse following the pump pulse after a delay time. (b) Chemical structure of canthaxanthin.

S_1 state, and these vibrationally excited molecules relax to a thermal equilibrium in tens of picoseconds.

Hayashi et al.[13] have reported the picosecond time-resolved anti-Stokes Raman spectra of vibrationally excited carotenoid molecules generated through the photoexcitation and relaxation processes mentioned above (Figure 1a). The frequencies of a few characteristic Raman bands in the 1600−900 cm^{-1} region as well as their intensities change on the time scale of picoseconds. This result has been interpreted as arising from generation of molecules on highly excited vibrational levels of high-frequency skeletal modes and their relaxation.[13] In order to understand the observed results in more detail, it is necessary to determine the energy levels on which the observed vibrationally excited molecules are populated.

In the preceding paper,[18] we have shown that anti-Stokes resonance Raman excitation profiles (REPs) are useful for determining the initial vibrational level from which the anti-Stokes Raman scattering occurs. In the present paper, we observe picosecond time-resolved anti-Stokes Raman spectra from molecules of canthaxanthin (a carotenoid whose chemical structure is depicted in Figure 1b) populated on vibrationally excited levels in the S_0 state. We determine the energy level(s) from which the observed anti-Stokes Raman scattering occurs, according to the method proposed in the preceding paper.[18] The vibrational relaxation process of this carotenoid is discussed on the basis of the observed results.

Experimental Section

The experimental setup is schematically shown in Figure 2. A beam from a frequency-doubled cw mode-locked Nd:YLF laser (Quantronix 4216D, wavelength 527 nm, repetition rate 82 MHz, average power 2 W, pulse duration 40 ps) was used to excite two synchronously-pumped dye lasers (Spectra-Physics/Quantronix 3500). Light pulses with ∼3 ps duration and ∼1 nJ pulse energy were obtained at a repetition rate of 82 MHz. The laser wavelength was tunable between 540 and 670 nm with rhodamine 560, rhodamine 590, or DCM dyes. The pulse duration of the dye laser output was always monitored by home-built SHG autocorrelators. Pulses from the dye lasers passed through dye amplifiers (Leonix), and amplified pulses with pulse energies of 5−50 μJ were obtained at a repetition rate of 1 kHz. The dye amplifiers, which consisted of three-stage dye cells, were excited by the second harmonic of the output from a cw

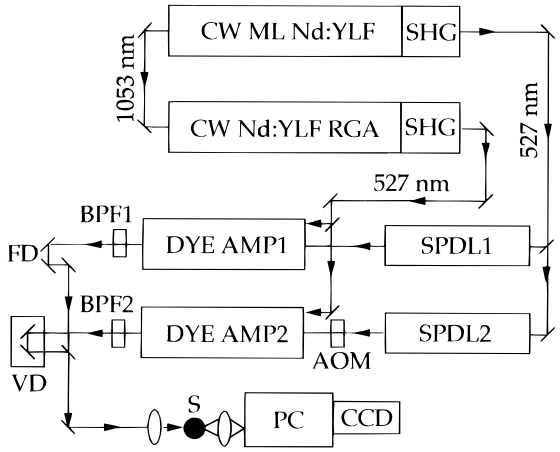

Figure 2. Block diagram of a picosecond time-resolved Raman spectrometer. CW ML Nd:YLF, cw mode-locked Nd:YLF laser; CW Nd:YLF RGA, cw Nd:YLF regenerative amplifier; SHG, second harmonic generator; SPDL, synchronously-pumped dye laser; AOM, acousto-optic modulator; DYE AMP, dye amplifier; BPF, bandpass filter; FD, fixed optical delay line; VD, variable optical delay line; S, sample; PC, polychromator; CCD, charge-coupled-device optical multichannel detector.

Nd:YLF regenerative amplifier (Quantronix 4417RG, 527 nm, 1 kHz, 1.2 W, 50 ps) seeded by the cw mode-locked Nd:YLF laser. The amplifying dyes used were rhodamine 590, rhodamine 610, or DCM, depending on the wavelength. The amplified dye-laser beams were used for the pump and probe fields in transient Raman measurements. To reduce the contribution of dye-laser pulses not amplified (82 MHz), an AO modulator (Isomet 1205C-2) was placed before the dye amplifier.

After being passed through fixed (for the pump beam) and variable (for the probe beam) optical delay lines, the pump and probe beams polarized in the same direction were superimposed by a half-mirror and focused onto the sample solution with a f = 50 or 70 mm lens. Narrow bandpass filters (CVI, spectral full width at half-maximum 10 nm) were used to eliminate fluorescence from the laser dyes. The sample solution was flowed through a 1 mm quartz cell. The average probe laser power was ∼0.1 mW for measurements of probe-wavelength dependence and 0.5−1 mW for measurements of delay-time dependence. The average power of the pump laser was ∼1 mW for both cases. For measurements of delay-time dependence, a feedback system[19] was used to reduce the timing jitter between the pump and probe pulses. As a result, time resolution (∼5 ps) was nearly determined by the duration of the pump and probe pulses.

The 90° scattered Raman signal was collected and dispersed by a triple polychromator (SPEX Triplemate 1877), and detected by a CCD detector (Princeton Instruments LN/CCD-1752PBU-VAR, 1752 × 532 pixels). The spectral slit width was ∼10 cm^{-1}. The typical exposure time was 10−60 min. Emission lines from a neon lamp were used to determine the wavelengths of the laser beams and to calibrate the Raman spectra. Canthaxanthin (Extrasynthèse) and benzene (Wako Pure Chemical Industries, special reagent grade) were used as received. The concentration of the sample solution was 1×10^{-4} mol dm^{-3}. All experiments were carried out at room temperature.

Results and Discussion

Delay-Time Dependence of Anti-Stokes Raman Spectra. Picosecond time-resolved anti-Stokes Raman spectra of canthaxanthin in a benzene solution are shown in Figure 3. The pump and probe wavelengths are 545 and 555 nm, respectively. The upper three spectra are recorded at delay times (between

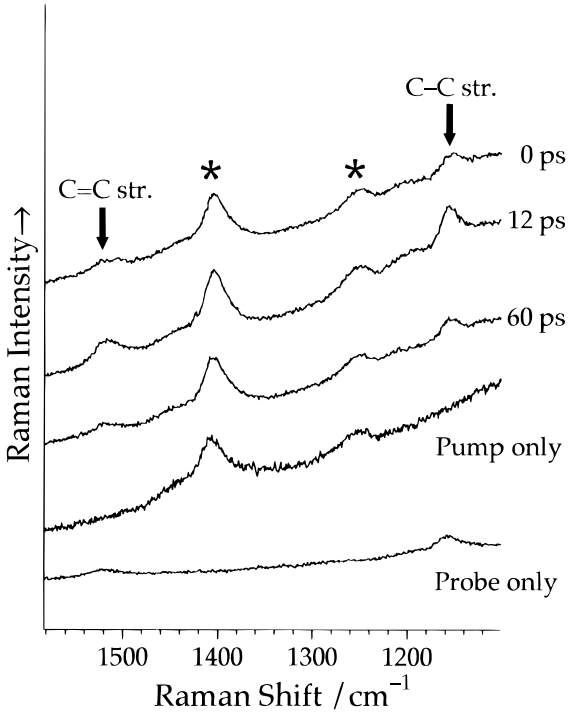

Figure 3. Anti-Stokes Raman spectra of canthaxanthin in a benzene solution. The delay time between the pump and probe pulses is given on the right of each spectrum. The two spectra at the bottom were obtained under the pump-only and the probe-only conditions, respectively. The Raman shift in the abscissa refers to that from the wavenumber of the probe laser light.

the pump and probe pulses) 0, 12, and 60 ps, respectively. The lower two are the pump-only and probe-only spectra. The background signal mostly arises from fluorescence emitted by the pump laser. In the time-resolved anti-Stokes Raman spectra, Raman bands due to the pump laser and those due to the probe laser are observed at the same time. Two Raman bands observed by the probe radiation (at 1520 and 1160 cm^{-1} from the probe frequency) are attributed to the "in-phase" C═C and C−C stretches of the S_0 canthaxanthin.[20,21] In addition, two Raman bands excited by the pump laser appear at the asterisked positions in Figure 3, which are attributed to the C−C stretch and methyl rock (at 1160 and 1005 cm^{-1} from the position of the pump frequency).[20,21]

In Figure 3, the intensities of the asterisked Raman bands due to the pump laser are independent of the delay time, while the pump-induced intensities observed by the probe laser show clear delay-time dependence. The pump-induced Raman intensities observed by the probe laser at delay time 12 ps are higher than those at delay times 0 and 60 ps. The intensity increase of the Raman bands at delay time 12 ps can be attributed to an increase in the populations of vibrationally excited transients in the S_0 electronic state generated via internal conversion from the S_1 state. Figure 4 shows the delay time dependence of the anti-Stokes Raman band at 1520 cm^{-1} (C═C stretch). A plot of the intensity of this Raman band against the delay time is shown in Figure 5. The anti-Stokes Raman intensity first rises in several picoseconds, reaches a maximum at ∼12 ps, and then decays with a time constant of 15−20 ps. In the region of negative time delays, spectra are almost the same as those arising from the thermally populated vibrationally excited molecules at room temperature, since the probe intensity is so weak that only a small portion of the whole molecules are excited by that. The C−C stretching Raman intensity shows the same temporal behavior. These results are consistent with the scheme of photophysical dynamics depicted in Figure 1a.

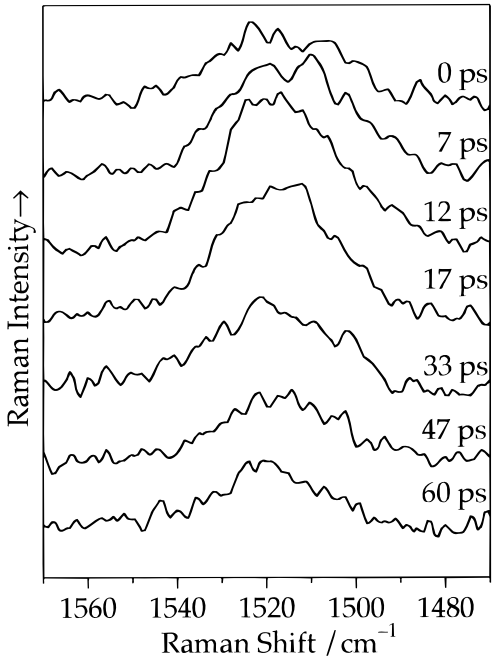

Figure 4. Temporal intensity change of the anti-Stokes Raman band at 1520 cm^{-1} of canthaxanthin (C═C stretch). The delay time between the pump and probe pulses is given on the right of each spectrum.

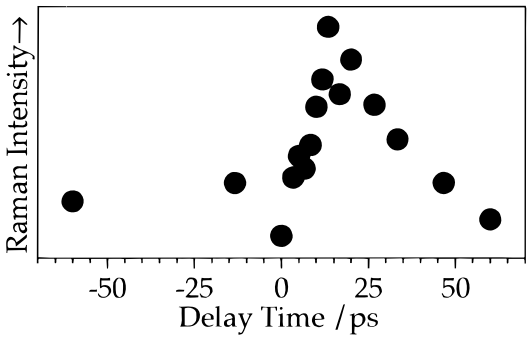

Figure 5. Plot of the anti-Stokes Raman intensity of the C═C stretching band at 1520 cm^{-1} of canthaxanthin against the delay time between the pump and probe pulses.

The rise of the anti-Stokes intensities reflects the generation of vibrationally excited molecules in the S_0 state via internal conversion from the S_1 state. The S_1 lifetime of canthaxanthin has been measured to be 5.2 ps by using picosecond time-resolved absorption spectroscopy.[22] This S_1 lifetime is in agreement with the delay time giving the maximum pump-induced Raman intensity (∼12 ps). The decay in Figure 5 reflects the vibrational relaxation toward a thermal equilibrium in S_0. The VC process is considered to be associated with this part. The decay rate is roughly the same as those of other carotenoids, i.e., spirilloxanthin,[13] decapreno-β-carotene,[23] and dodecapreno-β-carotene.[23] This suggests that the chain length and terminal groups have a minor effect on the decay rate. Whether the IVR process contributes to the observed temporal profiles of the anti-Stokes intensity or not will be discussed later.

The peak position of the C═C stretching Raman band also changes with the delay time. Figure 6a shows the difference between the spectra at delay times of 12 and 60 ps in the C═C stretching region. The band in this difference spectrum contains contributions downshifted by ∼5 cm^{-1} relative to the band maximum in the 60-ps delay spectrum (the band maximum in the 60-ps spectrum is equal to that in the stationary (cw) spectrum). This result indicates that the position of the transient C═C stretching Raman band shifts to a lower wavenumber from

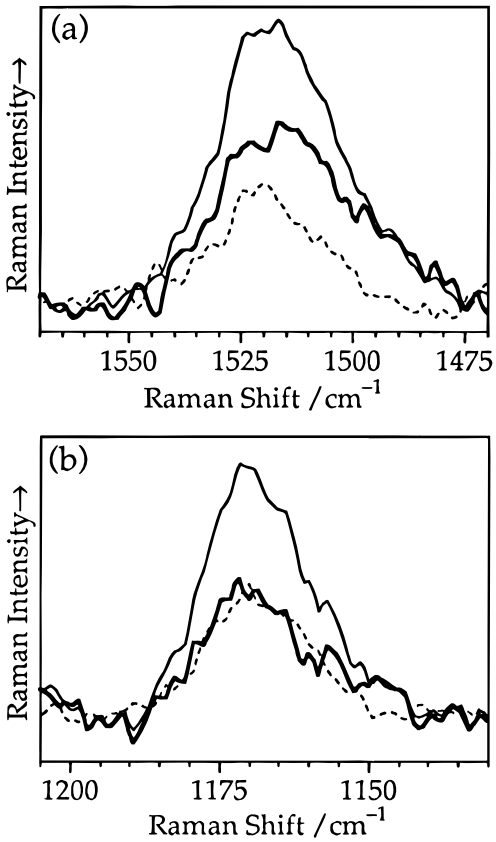

Figure 6. Anti-Stokes Raman spectra of canthaxanthin in the regions of the C═C stretch (a) and the C−C stretch (b). The thin solid and dotted traces are recorded at delay times 12 and 60 ps, respectively. The thick traces are the difference between the two spectra at delay times 12 and 60 ps.

that in the stationary spectrum. This observation is similar to that reported by Hayashi et al.[13] For the C−C stretching band, such a shift of the peak position is not observed clearly (Figure 6b). The separation between neighboring energy levels of the C═C stretch decreases with increasing vibrational quantum number.[21] It has been suggested[13] for other carotenoids that vibrationally excited transients with high quantum numbers about the C═C stretch are possibly probed in the pump−probe anti-Stokes Raman measurements. The molecular structures of linear polyenes in the S_1 states are believed to be significantly displaced along the C═C stretching coordinate from those of the S_0 states.[24,25] This seems to be consistent with the existence of high quantum number transients immediately after the internal conversion from the S_1 state. It is important to determine the energy states of the observed vibrationally excited transients more accurately to understand the photophysics of carotenoids and the mechanism of IVR. Thus, the probe-wavelength dependence of the intensity of the pump-induced C═C stretching anti-Stokes Raman band is observed and compared with simulated anti-Stokes REPs.

Probe-Wavelength Dependence of Pump-Induced Anti-Stokes Raman Intensity. The simulated anti-Stokes Raman excitation profiles of the C═C stretching band are shown in Figure 7 for various initial levels ($n_{C=C} = 1-6$). The method of simulation and the parameters used for the calculation are the same as those adopted in the preceding paper.[18] The anti-Stokes REPs are characteristic of individual initial levels. The intensity of the anti-Stokes Raman band arising from the lowest excited level ($n_{C=C} = 1$) decreases monotonically when the Raman excitation is performed at a wavelength longer than 555 nm. On the other hand, the intensity of anti-Stokes Raman bands arising from higher excited ($n_{C=C} \geq 3$) levels are expected

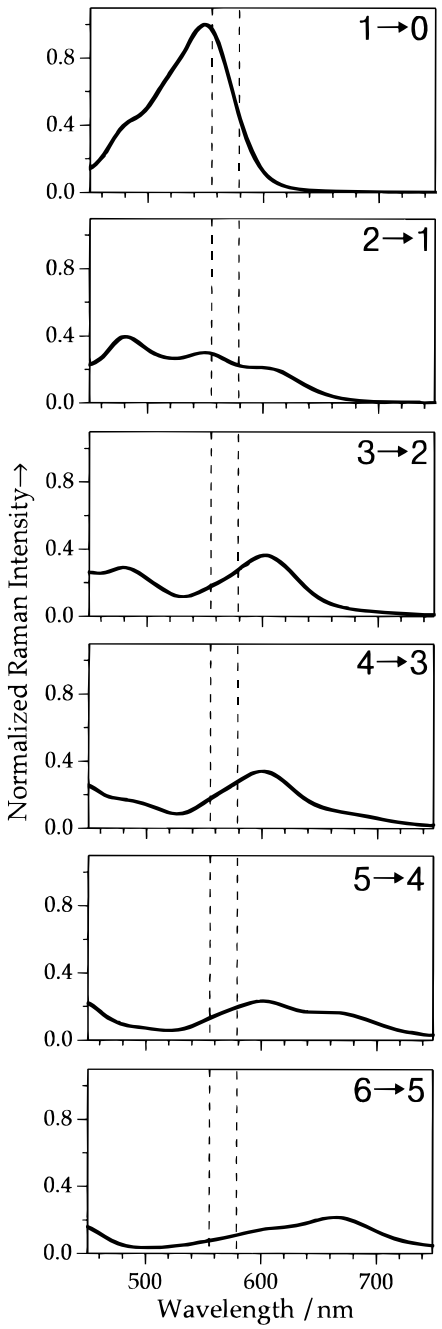

Figure 7. Simulated anti-Stokes Raman excitation profiles for the C═C stretching band at 1520 cm^{-1} of canthaxanthin for various initial levels of the C═C stretching mode.

to increase when a longer wavelength is adopted for Raman measurements. Consequently, it may be possible to distinguish molecules on the lowest excited level from those on the highly excited levels, if the anti-Stokes Raman intensity taken with the 555-nm probe light is compared with that probed by an appropriately longer wavelength.

In order to compare the anti-Stokes Raman intensities taken at two probe wavelengths, an internal intensity reference is needed. In the present experiment, the intensities of solvent Raman bands cannot be utilized as intensity references, because of their very weak anti-Stokes signals. Instead, we use the probe-only anti-Stokes Raman intensity as an intensity reference, which originates from thermally populated vibrationally excited levels. This idea is schematically depicted in Figure 8, where the anti-Stokes Raman bands (due to the C═C stretch) convoluted with Gaussian model functions are depicted. The solid and dotted curves represent the pump-on and the pump-

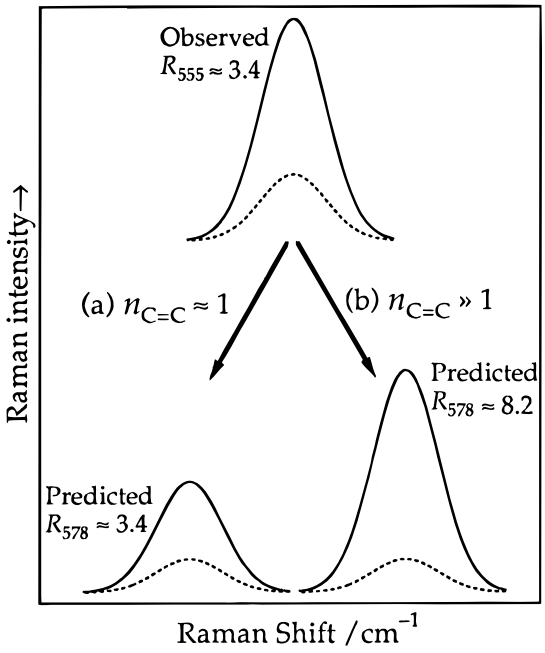

Figure 8. Simulated probe-wavelength dependence (555 and 578 nm) of the anti-Stokes Raman intensity of the C═C stretching band. The solid and dotted curves show the pump-on and the pump-off spectra, respectively. R_{555} and R_{578} represent the R values measured at 555 and 578 nm, respectively.

off (probe-only) spectra, respectively. Molecules giving rise to anti-Stokes Raman scattering at room temperature are mostly on the $n_{C=C} = 1$ level. Thus, the pump-off spectra show the intensity arising from the $n_{C=C} = 1$ level. We denote the pump-on/pump-off intensity ratio for probe-wavelength λ as R_λ. R_λ is given by the following equation:

$$R_\lambda = \frac{I_{Pr}{}^{\lambda} + I_{Tr}{}^{\lambda}}{I_{Pr}{}^{\lambda}} \quad (1)$$

where $I_{Pr}{}^{\lambda}$ and $I_{Tr}{}^{\lambda}$ denote the anti-Stokes Raman intensities from the thermally populated molecules and the pump-induced transients, respectively. The observed maximum R_λ value (∼12 ps) for 555-nm probe (R_{555}) is ∼3.4 (Figure 8), if the probe-laser intensity is kept as low as possible to avoid various unfavorable strong field effects.[26] From eq 1 and the R_{555} value (∼3.4), it is found that the anti-Stokes Raman intensity from the pump-induced transients ($I_{Tr}{}^{555}$) is ∼2.4 times as large as that from the thermally populated molecules ($I_{Pr}{}^{555}$). If the pump-induced transient is on the $n_{C=C} = 1$ level, the probe-wavelength dependence of anti-Stokes Raman intensity arising from the pump-induced transients should be the same as that arising from the thermally populated molecules (the pump-off spectra). In this case, R should be unchanged for any probe wavelength, although observed intensities themselves may change; for example, $R_{578} \approx 3.4$ as shown in Figure 8a. On the other hand, if the pump-induced transient is on a highly excited vibrational level, the anti-Stokes Raman intensity arising from the pump-induced transients is expected to increase with a longer probe wavelength. In that case, R should be increased for a probe wavelength longer than 555 nm. As is shown in Figure 7, for 578-nm probe, $I_{Pr}{}^{578}$ is half as large as $I_{Pr}{}^{555}$ ($I_{Pr}{}^{578} \approx 0.5 I_{Pr}{}^{555}$), while $I_{Tr}{}^{578}$ is ∼1.5 times as large as $I_{Tr}{}^{555}$ ($I_{Tr}{}^{578} \approx 1.5 I_{Tr}{}^{555}$), if all the pump-induced transients is on the $n_{C=C} \geq 3$ levels. From eq 1, R_{578} can be estimated to be ∼8.2 (Figure 8b).

On the basis of the above discussion, anti-Stokes Raman spectra are observed with 578-nm probe, and compared with the 555-nm probe spectra. The observed probe-wavelength dependence is shown in Figure 9. The dotted traces are the pump-off spectra, and the solid traces are the pump-on spectra at delay time 12 ps (as mentioned earlier, the anti-Stokes Raman intensity reaches a maximum at ∼12 ps after the incidence of the pump pulse). In evaluating the R value, we may disregard reabsorption of the scattered light by the solute and the wavelength dependence of the detection system, since we compare the pump-on and pump-off spectra at the same Raman shift with the same probe-wavelength. In Figure 9, the signal-to-noise ratios are not high because of the very weak scattering intensity. However, the R value seems to be independent of the probe wavelength ($R_{555} \approx 3.4$ and $R_{578} \approx 3.6$), and the observed R_{578} value is clearly far from 8. This result leads us to a conclusion that the pump-induced anti-Stokes Raman intensity observed in the present study does not arise from highly excited vibrational states with $n_{C=C} \geq 3$. The similar analysis would be possible for the C−C stretching band. Unfortunately, we have not succeeded in obtaining high-quality spectra in this region for the 578 nm probe, because of fluorescence arising from the pump laser.

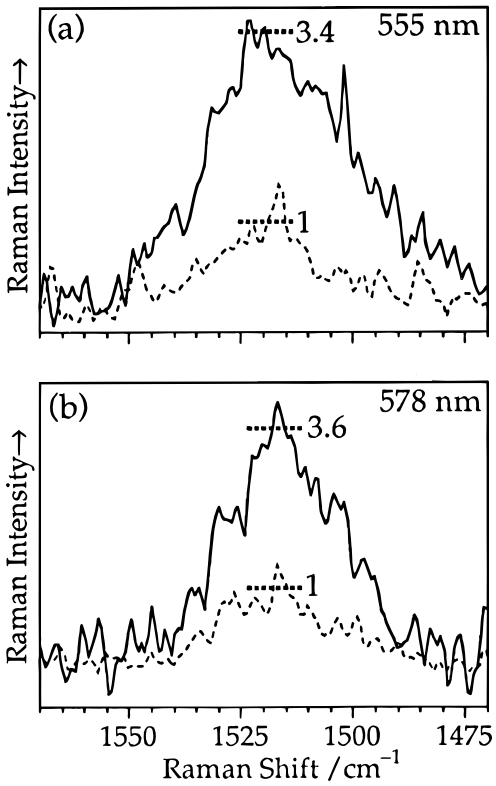

Figure 9. Observed probe-wavelength dependence of the anti-Stokes Raman intensity of the C═C stretching band. Probe wavelength, (a) 555 and (b) 578 nm. The upper trace in each panel represents the pump-on spectrum at delay time 12 ps and the lower trace the pump-off spectrum. The numbers in the figure indicate the ratios between the intensities of the solid and dotted curves.

In Figure 7, the anti-Stokes intensity from either the $n_{C=C} = 1$ or 2 level decreases when the probe wavelength is changed from 555 to 578 nm. This means that involvement of molecules on the $n_{C=C} = 2$ level may not be precluded by simply comparing the intensities observed with the two wavelengths (R_{578} is expected to be ∼4.5 in comparison with $R_{555} = 3.4$, if all the transient species are on the $n_{C=C} = 2$ level). If a probe light of a much longer wavelength (660 nm for example) is used, it may be possible to distinguish the contribution from molecules on the $n_{C=C} = 2$ level and that from molecules on the $n_{C=C} = 1$ level. The anti-Stokes intensity with 660-nm probe is predicted by the calculation (Figure 7) to be less than

1/100 of that with 555-nm probe, if the pump-induced transient species is on the $n_{C=C} = 1$ level, while it is ~1/5 if the transient species is on the $n_{C=C} = 2$ level. We can hence expect a large R value if the pump-induced transients are on the $n_{C=C} = 2$ level; $R_{660} \approx 50$ if all the transient species observed are on the $n_{C=C} = 2$ level, while R_{660} must be unchanged from R_{555} (~3.4) if they are on the $n_{C=C} = 1$ level.

The Stokes Raman scattering and fluorescence arising from the pump light (545 nm) overlaps with the anti-Stokes Raman scattering arising from the probe light around 660 nm, making it difficult to obtain a good quality anti-Stokes Raman spectrum. Nevertheless, it is found that (i) the absolute anti-Stokes intensity observed with the 660-nm probe light is far weaker than that observed with the 555-nm probe light and (ii) R_{660} does not seem to increase from R_{555}. These results suggest that molecules on the $n_{C=C} = 2$ level have only a small contribution, if any, to the observed pump-induced anti-Stokes Raman intensity.

The calculation predicts that the first-overtone anti-Stokes Raman band corresponding to the $n_{C=C} = 2$ to 0 process should have an intensity about half of that for the $n_{C=C} = 2$ to 1 process for 555-nm probe. If the pump-induced transients are on the $n_{C=C} = 2$ level, the first-overtone anti-Stokes Raman band must be observed and its intensity is expected to change with the delay time. The widths of overtone bands are generally broader than those of fundamental bands, making the observation of overtone bands more difficult. Actually, a very weak anti-Stokes Raman band is present at ~3040 cm^{-1}, but it is difficult to observe with certainty its delay-time dependence because of a poor signal-to-noise ratio.

Anti-Stokes Raman intensities arising from some levels of combination with other Franck−Condon active modes (C−C stretch and/or methyl rock) show probe-wavelength dependencies similar to that of the $n_{C=C} = 2$ to 1 process.[18] Contribution of such combination levels to the spectra observed in the present study is consequently considered to be minor for the same reasons about the $n_{C=C} = 2$ level. To summarize, for the "in-phase" C═C stretching mode, the observed vibrationally excited transients at delay time 12 ps are mostly in the lowest excited vibrational state ($n_{C=C} = 1$). However, whether the energy distribution is statistical or not is a question remaining at this stage. In the next subsection, we discuss this point in terms of the transient vibrational temperature and refer to the origin of the observed downshift of the C═C stretching band.

Intramolecular Vibrational Redistribution in Canthaxanthin. To examine whether vibrational excess energy is statistically distributed in the molecule or not, comparison is made between the transient vibrational temperature derived from the observed data and that calculated on the assumption of statistical distribution of the excess energy.

Firstly, the transient vibrational temperature is calculated on the assumption that the excess energy is statistically distributed among all the intramolecular vibrational modes. The relation between the transient vibrational temperature T_t and the excess energy thermally distributed among all the vibrational modes is given by the following equation:

$$\sum_{i=1}^{3N-6} \frac{h\nu_i \exp\left(-\frac{h\nu_i}{kT_r}\right)}{1-\exp\left(-\frac{h\nu_i}{kT_r}\right)} + \Delta E = \sum_{i=1}^{3N-6} \frac{h\nu_i \exp\left(-\frac{h\nu_i}{kT_t}\right)}{1-\exp\left(-\frac{h\nu_i}{kT_t}\right)} \quad (2)$$

where k, h, and T_r denote respectively the Boltzmann and the Planck constants and the room temperature (300 K). ΔE is the incident excess energy, and ν_i's ($i = 1, 2, ..., 3N - 6$) are the vibrational frequencies of canthaxanthin. Since it is hard to know precisely all the vibrational frequencies of canthaxanthin, we introduce an approximation that the vibrational modes of canthaxanthin (276 modes in total) lie at equal intervals between 0 and 1600 cm^{-1}, except for the C−H stretches (52 modes) which are assumed to have a single wavenumber of 3000 cm^{-1}.[7] The excess energy ΔE (which the canthaxanthin molecule has immediately after the internal conversion from S_1 to S_0) is given by the energy separation between the S_1 and S_0 states, which is taken to be ~15000 cm^{-1}.[16,23] The transient vibrational temperature T_t thus calculated is ~500 K.

Next, we estimate the transient vibrational temperature (at delay time 12 ps) from the experimental data, assuming the Boltzmann distribution. At a delay time of 12 ps, the pump-induced anti-Stokes intensity is mostly due to molecules on the $n_{C=C} = 1$ level as described in the previous subsection. Consequently, the transient temperature of vibrationally excited molecules, with respect to the C═C stretching mode, can be estimated from the observed R value (~3.4) and the excitation efficiency η (ratio of the number of excited molecules to that of all molecules in the probed volume). The pump-on anti-Stokes Raman intensity (I_{AP}) is assumed to be given by the following equation:

$$I_{AP} = (1 - \eta)I_A(T_r) + \eta I_A(T_t) \quad (3)$$

where $I_A(T)$ is the anti-Stokes Raman intensity at a given temperature T. $I_A(T_r)$ and $I_A(T_t)$ are obtained, respectively, as products of the corresponding Stokes intensities $I_S(T_r)$ and $I_S(T_t)$ and the Boltzmann factor

$$I_A(T_r) = \exp\left(-\frac{h\nu}{kT_r}\right) I_S(T_r)$$

$$I_A(T_t) = \exp\left(-\frac{h\nu}{kT_t}\right) I_S(T_t) \quad (4)$$

where ν denote the frequency of the vibrational mode under study. Since R is given by $I_{AP}/I_A(T_r)$, the following equation is derived.

$$\frac{1}{T_t} = \frac{1}{T_r} - \frac{k}{h\nu}\left(\ln\left(\frac{I_S(T_r)}{I_S(T_t)}\right) + \ln\left(\frac{1}{\eta}(R + \eta - 1)\right)\right) \quad (5)$$

The factor $\ln[I_s(T_r)/I_s(T_t)]$ is negligibly small, since the Stokes intensity ratio $I_s(T_r)/I_s(T_t)$ is nearly equal to 1. The value of η is estimated to be ~0.1, on the basis of our typical experimental conditions (concentration, 1×10^{-4} mol dm^{-3}; spot area, 1×10^{-3} cm^{-2}; pass length, 1 mm; absorption coefficient, 1×10^4 mol^{-1} cm^{-1} dm^3; pulse energy, 1×10^{-6} J; pump laser wavenumber, 18350 cm^{-1}). Consequently, T_t is found to be ~540 K, if we substitute $\nu = 1520$ cm^{-1} and $T_r = 300$ K. This value is close to the theoretically calculated one (~500 K), in view of the uncertainties of the calculated and experimental values. Thus, we conclude that the excess vibrational energy in canthaxanthin is, at least for the major part, statistically distributed among all the intramolecular vibrational modes with a time constant of redistribution much shorter than 12 ps. It may now be concluded that contribution of the IVR process lies, if any, in the rise part of the observed time dependence of the anti-Stokes Raman intensity in Figure 5, and cannot be distinguishable from the $S_1 \rightarrow S_0$ electronic relaxation. Only the VC process contributes to its decay part.

The result mentioned in the previous subsection that the transient species at delay time 12 ps are populated on the $n_{C=C}$

= 1 level seems to be contradictory to the experimental observation that the Raman band at ~1520 cm^{-1} is shifted to a slightly lower frequency at the same delay time. As mentioned earlier, the S_0 transients immediately after internal conversion from S_1 to S_0 are considered to be highly excited about the C=C stretching mode. The present result suggests that the localized vibrational energy is very rapidly redistributed among the entire vibrational modes in the molecule. Since the excess energy localized in the C=C stretching mode is redistributed very rapidly, many other modes including Raman-inactive dark modes and low-frequency modes are excited. Vibrational excitation of these modes may be substantially high as a whole. Consequently, the observed pump-induced C=C stretching anti-Stokes Raman intensity arises from the (1,*n*) to (0,*n*) process, where the first index refers to the vibrational quantum number of the C=C stretching mode and the second one the summation of the vibrational quantum numbers of some other modes that are anharmonically coupled with the C=C stretching mode.[27,28] Since such anharmonicity coupling is expected to decrease the energy spacing between the (1,*n*) and (0,*n*) states in comparison with that between the (1,0) and (0,0) states, the peak position of the C=C stretching Raman band shift to a lower wavenumber at delay time 12 ps. A similar situation must be present in the cases of other carotenoids (*in vivo* and in solution) reported by Hayashi et al.,[13] although dynamic features (rise time, magnitude of the low-frequency shift, etc.) observed in their study are different from those in the present case. The above consideration on anharmonicity coupling suggests that the observed frequency shifts are not useful to discuss quantitatively the transient vibrational levels. It is very difficult to eliminate the thermal effects[9,27,28] from the observed frequency shifts, since temperature dependence of the observed frequency, which is closely related to the anharmonic coupling with low-frequency modes, cannot be predicted quantitatively.

In summary, we have studied the vibrational relaxation process of the S_0 state of canthaxanthin after the internal conversion from the S_1 to the S_0 state using the picosecond time-resolved anti-Stokes Raman spectroscopy. Comparison of the probe-wavelength dependence of the transient anti-Stokes Raman spectra with the simulated anti-Stokes Raman excitation profiles has shown that the IVR process of the S_0 state of canthaxanthin is very fast and the vibrationally excited transients giving rise to the transient 1520-cm^{-1} band at a delay time giving the maximum pump-induced Raman intensity are mostly in the first excited vibrational state of the C=C stretching mode. Finally, we conclude that the analysis of time-resolved anti-Stokes resonance Raman excitation profiles provides important information on vibrational relaxation processes. Results obtained by applying this method to *trans*-stilbene in the S_1 state will be reported elsewhere.

References and Notes

(1) Elsaesser, T.; Kaiser, W. *Annu. Rev. Phys. Chem.* **1991**, *42*, 83.
(2) Sension, R. J.; Szarka, A. Z.; Hochstrasser, R. M. *J. Chem. Phys.* **1992**, *97*, 5239.
(3) Sension, R. J.; Repinec, S. T.; Szarka, A. Z.; Hochstrasser, R. M. *J. Chem. Phys.* **1993**, *98*, 6291.
(4) Qian, J.; Schultz, S. L.; Jean, J. M. *Chem. Phys. Lett.* **1995**, *233*, 9.
(5) Matousek, P.; Parker, A. W.; Toner, W. T.; Towrie, M.; de Faria, D. L. A.; Hester, R. E.; Moore, J. N. *Chem. Phys. Lett.* **1995**, *237*, 373.
(6) Doig, S. J.; Reid, P. J.; Mathies, R. A. *J. Phys. Chem.* **1991**, *95*, 6372.
(7) Shreve, A. P.; Mathies, R. A. *J. Phys. Chem.* **1995**, *99*, 7285.
(8) Schneebeck, M. C.; Vigil, L. E.; Ondrias, M. R. *Chem. Phys. Lett.* **1993**, *215*, 251.
(9) Sato, S.; Kitagawa, T. *Appl. Phys. B* **1994**, *59*, 415.
(10) Lenz, K.; Pfeiffer, M.; Lau, A.; Elsaesser, T. *Chem. Phys. Lett.* **1994**, *229*, 340.
(11) Todd, D. C.; Fleming, G. R.; Jean, J. M. *J. Chem. Phys.* **1992**, *97*, 8915.
(12) Phillips, D. L.; Rodier, J.-M.; Myers, A. B. *Chem. Phys.* **1993**, *175*, 1.
(13) Hayashi, H.; Brack, T. L.; Noguchi, T.; Tasumi, M.; Atkinson, G. H. *J. Phys. Chem.* **1991**, *95*, 6797.
(14) Siefermann-Harms, D. *Biochim. Biophys. Acta* **1985**, *811*, 325.
(15) Cogdell, R. J.; Frank, H. A. *Biochim. Biophys. Acta* **1987**, *895*, 63.
(16) Koyama, Y.; Kuki, M.; Andersson, P. O.; Gillbro, T. *Photochem. Photobiol.* **1996**, *63*, 243.
(17) Frank, H. A.; Cogdell, R. J. *Photochem. Photobiol.* **1996**, *63*, 257.
(18) Okamoto, H.; Nakabayashi, T.; Tasumi, M. *J. Phys. Chem. A* **1997**, *101*, 3488.
(19) Okamoto, H.; Tasumi, M. *Rev. Sci. Instr.* **1995**, *66*, 5165.
(20) Hashimoto, H.; Koyama, Y. *Photochem. Photobiol.* **1991**, *54*, 67.
(21) Okamoto, H.; Sekimoto, Y. Tasumi, M. *Spectrochim. Acta* **1994**, *50A*, 1467.
(22) Wasielewski, M. R.; Kispert, L. D. *Chem. Phys. Lett.* **1986**, *128*, 238.
(23) Andersson, P. O.; Gillbro, T. *J. Chem. Phys.* **1995**, *103*, 2509.
(24) Zerbetto, F.; Zgierski, M. Z.; Negri, F.; Orlandi, G. *J. Chem. Phys.* **1988**, *89*, 3681.
(25) Aoyagi, M.; Kohler, B. E.; Ohmine, I. *J. Phys. Chem.* **1990**, *94*, 3922.
(26) Iwata, K.; Hamaguchi, H. *J. Raman Spectrosc.* **1994**, *25*, 615.
(27) Asher, S. D.; Murtaugh, J. *J. Am. Chem. Soc.* **1983**, *105*, 7244.
(28) Hester, R. E.; Matousek, P.; Moore, J. N.; Parker, A. W.; Toner, W. T.; Towrie, M. *Chem. Phys. Lett.* **1993**, *208*, 471.